Acyl Carrier Protein Phosphodiesterase (AcpH) of *Escherichia coli* Is a Non-Canonical Member of the HD Phosphatase/Phosphodiesterase Family†

Jacob Thomas,‡ Daniel J. Rigden,‖ and John E. Cronan*,‡,§

Departments of Microbiology and Biochemistry, University of Illinois at Urbana−Champaign, Urbana, Illinois 61801, and School of Biological Sciences, University of Liverpool, Liverpool L69 7ZB, U.K.

Received August 29, 2006; Revised Manuscript Received November 4, 2006

ABSTRACT: The *Escherichia coli* AcpH acyl carrier protein phosphodiesterase (also called ACP hydrolyase) is the only enzyme known to cleave a phosphodiester-linked post-translational protein modification. AcpH hydrolyzes the link between 4′-phosphopantetheine and the serine-36 side chain of acyl carrier protein (ACP). Although the existence of this enzyme activity has long been known, study of the enzyme was hampered by its recalcitrant properties and scarcity. We recently isolated the gene encoding AcpH and have produced the recombinant enzyme in quantity (Thomas, J., and Cronan, J. E., (2005) *J. Biol. Chem. 280,* 34675−34683), thus allowing the first studies of its reaction mechanism. AcpH requires Mn^{2+} for activity, and thus, we focused on the metal binding ligands in order to locate the active site. Bioinformatic investigations indicated that AcpH and its homologues were weakly related to a phosphodiesterase of known structure, the hydrolyase domain of the bifunctional bacterial protein, SpoT, suggesting that AcpH is a member of the HD family of phosphatases/ phosphodiesterases despite lacking the characteristic histidine of the motif. Indeed, we found that AcpH could be convincingly modeled on the SpoT structure with acceptable parameters, which allowed the identification of putative metal binding ligands. These were then tested by site-directed mutagenesis. Mutagenic removal of any of the putative ligands resulted in a severe or total loss of phosphodiesterase activity. In two cases, the H6Q and D24N proteins, the residual activities could be markedly stimulated by addition of high Mn^{2+} concentrations, thereby demonstrating a role for these residues in metal binding. We conclude that AcpH is a member of the HD protein family despite the lack of the signature histidine residue.

4′-Phosphopantetheine (4′-PP[1]), which is essentially the non-nucleotide portion of CoA, is covalently attached to a family of proteins that are very widely distributed throughout biology (*1*). The paradigm 4′-PP-modified proteins are the acyl carrier proteins (ACPs) of bacterial fatty acid synthesis where the sulfhydryl group of the 4′-PP moiety carries the growing fatty acid chain (*1*, *2*). In addition to bacteria, ACPs are found in plant plastids (*3*), mitochondria (*4*, *5*), and the apicoplasts of apicomplexan parasites (*6*). Other 4′-PP-modified proteins are found in polyketide and nonribosomal polypeptide synthesis, where these proteins (called PKS ACPs, and PCPs, respectively) perform analogous carrier functions (*1*). The PKS ACP and PCP proteins have the same general four-helix bundle structure found in bacterial ACPs. The 4′-PP moiety is attached to the apo form of ACP and its homologues by transfer from CoA catalyzed by enzymes called 4′-phosphopantetheine transferases that fall into at least three classes based on the specificities and quarternary structures of the proteins (*1*, *7*, *8*).

Given the key metabolic role of ACP in lipid synthesis, it is surprising that Gram-negative bacteria contain an enzyme that removes the 4′-PP moiety from *Escherichia coli* ACP to give the inactive apo form of ACP and free 4′-PP as products (*9*). Although this enzyme, first called ACP hydrolase (AcpH) and then ACP phosphodiesterase, was demonstrated almost 40 years ago (*9*), the identification of the encoding gene (called *acpH*) and production of the recombinant protein has only recently been accomplished (*10*). Hence, the mechanism of the enzyme has not been studied, except that the reaction is known to require divalent cations of which Mn^{2+} is the most efficient activator (*9*, *11*). Although many other phosphodiesterases have been studied, to our knowledge, all of these act on small molecule substrates. AcpH is the only enzyme known to cleave a protein-bound phosphodiester. We report here bioinformatic, modeling, and mutagenesis studies indicating that AcpH is a noncanonical member of the HD superfamily of phosphatases.

EXPERIMENTAL PROCEDURES

Bioinformatics and Modeling. Sequences homologous to *E. coli* AcpH and later to homologues of *Streptococcus dysgalactiae* SpoT were sought in the GenPept database at the National Center for Biotechnology Information (NCBI)

† This work was supported by National Institutes of Health Grant No. AI15650.

* Corresponding author. Phone: 217-333-7919. Fax: 217-244-6697. E-mail: j-cronan@life.uiuc.edu.

‡ Department of Microbiology,University of Illinois at Urbana−Champaign.

§ Department of Biochemistry, University of Illinois at Urbana−Champaign.

‖ University of Liverpool.

[1] Abbreviations: ACP, acyl carrier protein; 4′-PP, 4′-phosphopantetheine.

10.1021/bi061789e CCC: $37.00
Published on Web 01/02/2007

Table 1: Bacterial Strains, Plasmids, and Oligonucleotides

strain or plasmid	relevant characteristics	source
	strains	
MG1655	wild type	lab collection
MC1061	*araD139* Δ*(ara-leu)7696* Δ*(lac)X74 rpsL hsdR2*	(*33*)
SJ16	*panD2 zad-220::Tn*10 *relA1 spoT1 metB*	(*34*)
JT1	MC1061 *acpH*::*cat*	(*10*)
JT37	MG1655 *acpH*::*cat*	this work
JT38	MG1655 Δ*acpH*	this work
	plasmids	
pKK223-3	Amp^r expression vector, *tac* promoter	*Pharmacia*
pMS421	$Spec^r$; encodes $LacI^q$	(*27*)
pMR19	Amp^r, synthetic *acpP* under *tac* promoter control	(*28*)
pCP20	Amp^r Cm^r, Rep^{ts}, encodes FLP recombinase	(*23*)
pJT40	Encodes hexahistidine tagged AcpH under *tac* control in pKK223−3	this work
pJT41	Encodes AcpH H6Q; site-directed mutagenesis of pJT40	this work
pJT42	Encodes AcpH D24N; site-directed mutagenesis of pJT40	this work
pJT43	Encodes AcpH D78N; site-directed mutagenesis of pJT40	this work
pJT44	Encodes AcpH D82N; site-directed mutagenesis of pJT40	this work
pJT49	Encodes AcpH Δ2-6;site-directed mutagenesis of pJT40	this work
pJT57	Encodes AcpH A23H; site-directed mutagenesis of pJT40	this work
pJT58	Encodes AcpH H6Q H8Q; site-directed mutagenesis of pJT40	this work

Oligonucleotides

primer	sequence (5′−3′)
EcoAcpHFor	CCGAATTCTAAGGAGGAGACCAATGAATTTTTTAGCTCACCTGC
PstAcpHRev	GGGACCCTGCAGTTAATGATGATGATGATGATGTAACGCCTTGCGTGACGCC
EcoNTDelAcpHFor	CCGAATTCTAAGGAGGAGACCAATGCATTTAGCCCATCTCGCG
AcpHH6QFor	CCAATGAATTTTTTAGCTCAGCTGCATTTAGCCCATCTCG
AcpHH6QRev	CGAGATGGGCTAAATGCAGCTGAGCTAAAAAATTCATTGG
AcpHH6QH8QFor	CCAATGAATTTTTTAGCTCAGCTGCAGTTAGCCCATCTCGCGG
AcpHH6QH8QRev	CCGCGAGATGGGCTAACTGCAGCTGAGCTAAAAAATTCATTGG
AcpHA23HFor	CCGGCAATTTACTGCATGATTTCGTACGCGGAAATCCTG
AcpHA23HRev	CAGGATTTCCGCGTACGAAATCATGCAGTAAATTGCCGG
AcpHD24NFor	CCGGCAATTTACTGGCTAATTTCGTACGCGGAAATC
AcpHD24NRev	GATTTCCGCGTACGAAATTAGCCAGTAAATTGCCGG
AcpHD78NFor	GTTGCGCCTATTACGCTGAATGTCATGTGGGATCAC
AcpHD78NRev	GTGATCCCACATGACATTCAGCGTAATAGGCGCAAC
AcpHD82NFor	GCTGGATGTCATGTGGAATCACTTTCTTTCCCGC
AcpHD82NRev	GCGGGAAAGAAAGTGATTCCACATGACATCCAGC

using BLAST and PSI-BLAST (*12*), and the resulting sequence set was aligned using MUSCLE (Edgar, 2004). The five maximally disparate representatives of each set were determined using Jalview (*13*), which was also used for general alignment visualization and manipulation. Modeling was carried out with MODELLER (*14*), with PROCHECK (*15*) used for stereochemical validation of the models. ESPRIPT (*16*) was used for mapping conserved sequences onto structures. Several diverse putative ACP phosphodiesterase sequences were submitted to the META server (*17*), a portal to the leading fold recognition methods for consensus predictions of maximized reliability (ref 18 (*18*) and refs therein). The most informative results in this case came from the Meta-BASIC method, a sensitive tool that serves to align sequence profiles pairwise in combination with their predicted secondary structures (*19*). Predictions were also made with HHpred (*20*, *21*). Secondary structures were predicted using PSI-PRED (*22*).

Materials. Oligonucleotides for PCR and site-directed mutagenesis were purchased from IDT (Coralville, IA). QuikChange site-directed mutagenesis kits and *Pfu* DNA polymerase were from Stratagene (LaJolla, CA). Restriction enzymes and T4 DNA ligase were from New England Biolabs (Beverly, MA). Protein folding columns were obtained from Profoldin (Westborough, MA). Vivaspin D (diethylaminoethyl) columns were purchased from Sartorius (Edgewood, NY). Molecular biology reagents were from Qiagen (Valencia, CA). β-[3-^3H]Alanine was from American Radiolabeled Chemicals (St Louis, MO). All other chemicals were from Sigma-Aldrich.

Bacterial Strains and Plasmids. Bacterial strains and plasmids are listed in Table 1. All strains used were derivatives of *E. coli* K-12. Strain JT37 was constructed by using a P1*vir* lysate made on strain JT1 (*10*) to transduce strain MG1655 to chloramphenicol resistance. The resistance cassette was then excised using FLP recombinase expressed from the plasmid pCP20 (*23*, *24*) to give strain JT38. Plasmid pJT40, which expresses the hexahistidine tagged AcpH from a *tac* promoter, was constructed by first PCR amplifying the *acpH* gene from strain MG1655 genomic DNA using primers EcoAcpHFor and PstAcpHRev (Table 1). The PCR product was then digested with EcoRI and PstI and ligated into the expression vector pKK223-3 (Pharmacia Biotech) digested with the same enzymes. Plasmid pJT49, which encodes a hexahistidine-tagged *N*-terminally truncated AcpH lacking amino acids 2−6 of the native protein, was constructed in the same manner using primers EcoNTdelAcpHFor and PstAcpHRev. The plasmids encoding single-residue substitu-

tions were constructed using the QuikChange site-directed mutagenesis kit (Stratagene), according to the manufacturer's instructions, using the primers listed in Table 1 and plasmid pJT40 as the template. The inserts of all plasmids constructed were sequenced at the Keck Biotechnology Center, University of Illinois to verify the mutations introduced. All strains were cultured on LB medium at 37 °C. For the purification of tritiated ACP, strain DK574 (*25*) was cultured on minimal medium E (*26*) supplemented with 0.4% glucose and 0.1% Casamino acids. When required for plasmid maintenance, ampicillin and spectinomycin were used at a concentration of 100 μg/mL, chloramphenicol at 25 μg/mL, and kanamycin at 50 μg/mL.

Purification of AcpH Proteins. AcpH was purified using a procedure modified from that described previously (*10*). Derivatives of strain JT38 transformed with the LacI^q expression plasmid pMS421 (*27*) and a plasmid expressing a hexahistidine-tagged wild-type or mutant AcpH species were subcultured from an overnight culture into 50 mL of LB supplemented with ampicillin and spectinomycin. When the culture reached an OD_{600} of 0.8, it was induced with 200 μM isopropyl-β-D-thiogalactopyranoside for a further 2 h. The cells were harvested, washed with an equal volume of a pH 8.0 buffer containing 100 mM NaH_2PO_4 and 10 mM Tris-HCl, and then resuspended in 5 mL of the same buffer with the addition of 8 M urea. The cells were lysed by shaking at this suspension at room temperature for 1 h and then centrifuged at 14 000 rpm for 30 min. The supernatant was applied to a Ni-NTA column, which was then washed with 10 mL of 100 mM NaH_2PO_4, 10 mM Tris-HCl, and 8 M urea (pH 6.3) followed by 10 mL of 100 mM NaH_2PO_4, 10 mM Tris-HCl, and 8 M urea (pH 5.9). The hexahistidine-tagged protein was then eluted with 5 mL of an elution buffer of 100 mM NaH_2PO_4, 10 mM Tris-HCl, and 8 M urea (pH 4.5). The sample volume was decreased to 0.5 mL using Amicon centrifugal filters, and the denatured protein was refolded using Profoldin soluble protein folding column No. 10 according to the manufacturer's instructions. The mutant enzymes were purified in the same manner.

Purification of ACP. Holo-ACP was purified by a modification of the previous procedure (*25*). Briefly, strain DK574 (*25*), which is strain SJ16, harboring plasmids pMS421 (*27*) and pMR19 (*28*), was grown in LB medium to an OD_{600} of 0.8. The expression of ACP was then induced by the addition of 15 μM isopropyl-β-D-thiogalactopyranoside, and the culture was incubated for a further 3 h. Cells were harvested by centrifugation, washed with an equal volume of 50 mM potassium-MES at pH 6.1 (lysis buffer). The cells were then lysed by sonication in 0.1 volume of the same buffer. The crude lysate was mixed with an equal volume of ice-cold isopropanol and mixed by stirring at 4 °C for 1 h. This mixture was centrifuged and the supernatant applied to a Vivaspin D spin column (Sartorius) equilibrated with lysis buffer. The column was washed with 10 mL of lysis buffer and then with a further 10 mL of wash buffer (50 mM potassium 2-(*N*-morpholine)-ethane sulfonic acid and 0.25 M lithium chloride at pH 6.1). Holo-ACP was eluted with 0.5 M lithium chloride in 50 mM potassium 2-(*N*-morpholine)-ethane sulfonic acid (pH 6.1) and precipitated by the addition of sodium deoxycholate to 0.02% and trichloroacetic acid to 5%. The precipitate was incubated on ice for 30 min, washed with 1% trichloroacetic acid, and resuspended in 0.5 M Tris-HCl (pH 8.0). This solution was dialyzed against 20 mM Tris-HCl (pH 8.0) containing 1 mM dithiothreitol, and the purity of the samples was verified by electrophoresis on nondenaturing polyacrylamide gels (*10*). Holo-ACP labeled in the 4′-PP group was purified in the same manner except that strain DK574 was cultured overnight in minimal medium supplemented with 0.5 μM β-alanine to reduce the intracellular coenzyme A pools. This culture was then subcultured into minimal medium supplemented with 8 μM β-[3-^3H]-alanine (6.25 Ci/mmol) followed by induction of ACP expression and purification of protein as described above.

ACP Phosphodiesterase Assays. AcpH assays were performed as described previously (*10*). The reaction mixtures typically contained 20 μM holo-ACP, 0.1−2 pmol AcpH, 50 mM Tris-HCl (pH 8.5), 25 mM $MgCl_2$, 200 μM $MnCl_2$, and 1 mM dithiothreitol in a final volume of 50 μL. The assays were initiated by the addition of AcpH and incubated at room temperature for 1 to 2 h. When unlabeled holo-ACP was used as the substrate, the reactions were stopped by the addition of 10 μL of 100 mM EDTA, and the reaction products were separated by electrophoresis on nondenaturing acrylamide gels and visualized by Coomassie Blue staining. When [^3H]-ACP was used as a substrate, the reactions were stopped and protein precipitated by the addition of 20 μL of 20% trichloroacetic acid plus 10 μL of 5% bovine serum albumin as a co-precipitant. The reaction products were chilled on ice for 30 min and then centrifuged at 14 000 rpm for 30 min. The supernatant was extracted with 200 μL of water-saturated diethyl ether by vortex mixing to remove the trichloroacetic acid, and the aqueous phase was mixed with 5 mL of scintillation fluid and counted for radioactivity in a Beckman 6500 LS scintillation counter.

Kinetic Analyses. AcpH assays were performed as described above, using [^3H]-ACP (0.243 Ci/mmol) as the substrate at varying concentrations. Michaelis−Menten curves were fitted to experimental data by nonlinear regression using Origin software (Microcal) to obtain kinetic constants.

RESULTS

Modeling of AcpH on the SpoT Domain Structure. ACP phosphodiesterases are part of the Pfam family presently known as DUF479 (Domain of Unknown Function 479). There is no structure available for this family, and simple sequence searches with PSI-BLAST reveal no distant evolutionary relationships that might provide information about its structure. We felt that in order to probe the AcpH structure−function relationship, even an approximate structure would be very useful. We, therefore, submitted ACP phosphodiesterase sequences of DUF479 to both the HHpred and META servers, each capable of detecting less obvious evolutionary connections between protein families. In general, HHPred and the individual methods accessed through the META servers gave only poor scores to known structures with different protein architectures having similar scores. The exception, however, was METAbasic, which, although the top scores produced were of only medium significance, favored the one fold *N*-terminal domain of SpoT (*29*) (pdb code 1vj7) much more than any other. For example, the *E. coli* AcpH sequence matched SpoT with a score of 6.5, well ahead of the next hit at 2.1. This putative structural match

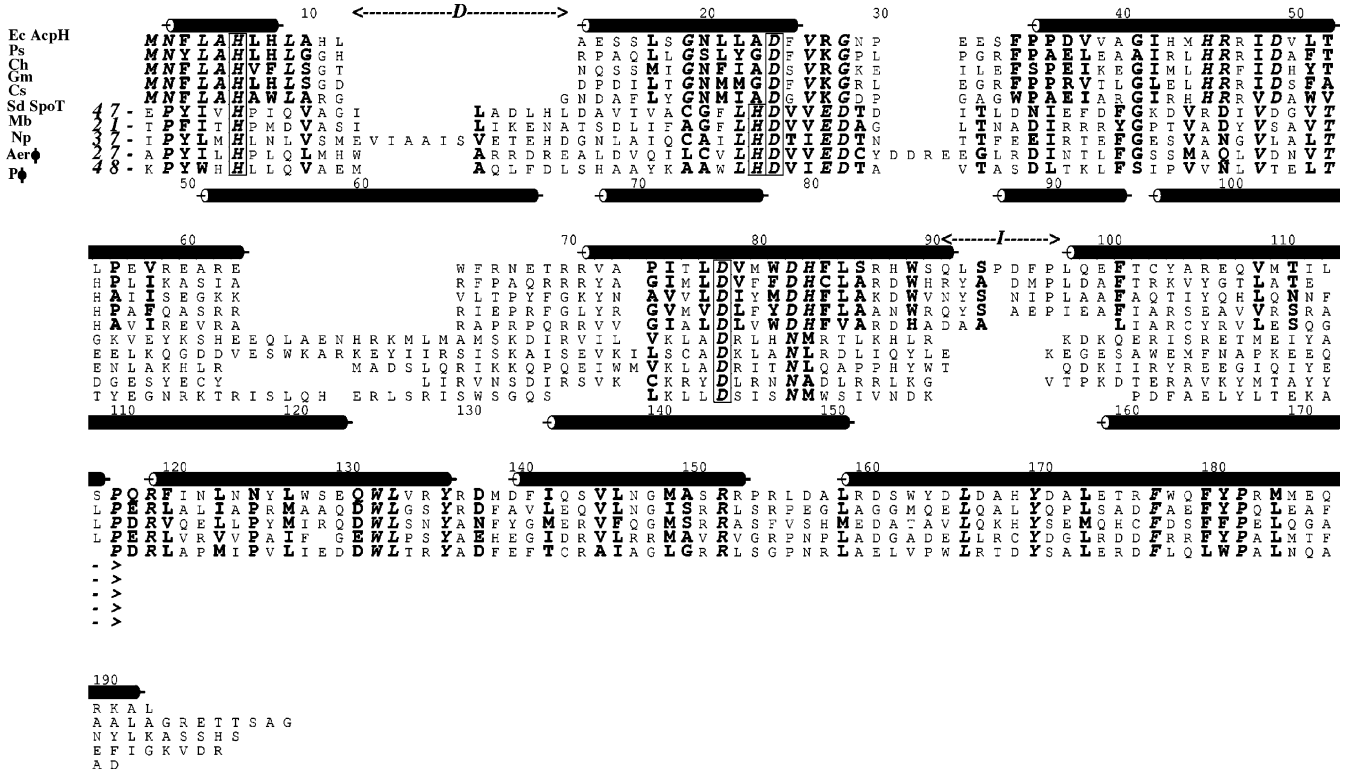

FIGURE 1: Alignment of sets of five maximally diverse sequences of ACP phosphodiesterase (above) with SpoT *N*-terminal domains (below). The abbreviated species names and the GenBank ID codes (in parentheses) of the corresponding sequences are Ec, *E. coli* (75238731); Ps, *Pseudomonas syringae* (28871491); Ch, *Cytophaga hutchinsonii* (48853925); Gm, *Geobacter metallireducens* (48845903); Cs, *Chromohalobacter salexigens* (67519571); Mb, *Methanococcoides burtonii* (53731505); Np, *Nostoc punctiforme* (23128993); Aerϕ, *Aeromonas* phage 44RR2.8t (23128993); and Pϕ, *Pseudomonas* phage ϕKZ (18996711). Above the alignment are the numbering and the predicted secondary structure for *E. coli* AcpH (*10*). The numbering of *S. dysgalactiae* SpoT and its observed secondary structure (pdb code 1vj7; (*29*)) are shown below the alignment. Conserved residues are in bold type, and invariant positions are additionally italicized. The boxes mark metal binding residues either known (*29*) or inferred from bioinformatics and site-directed mutagenesis. The *N*-terminal portion of SpoT, for which there is no homologue in AcpH, is indicated by the numbers of residues preceding the illustrated sequences. Similarly, the *C*-terminal remainder of SpoT, which cannot be aligned to ACP phosphodiesterase, even within the rest of its HD domain, is not shown. *I* and *D* mark the positions of the major insertion and deletion in AcpH relative to SpoT. The Figure was created with ALSCRIPT (*35*).

initially drew our attention because the *N*-terminal domain of SpoT also catalyzes a similar reaction, guanosine-3′, 5′-bis(diphosphate) 3′-diphosphatase. The SpoT *N*-terminal domain belongs to the HD superfamily of phosphatases, which also contains many enzymes having phosphodiesterase activity (*30*). We also noted that the activities of both enzymes depend on the Mn^{2+} ion (*11*, *29*). The alignment of the two families matches three of the four metal ligands of the SpoT domain with highly conserved residues of the ACP phosphodiesterase family, which seemed strong candidates to be metal-binding ligands (Figure 1). Moreover, there was a good correspondence between the predicted secondary structure of ACP phosphodiesterases and the known secondary structure of the SpoT domain (Figure 1).

Nevertheless, in the alignment of one family compared to the other, there were some substantial insertions and deletions, and the AcpH family members lacked a substantial *N*-terminal portion of the SpoT domain structure. In order to visualize the structural consequences of these differences, we constructed a model of the catalytic domain of *E. coli* AcpH on the basis of a minimally manually modified version of the alignment between it and *S. dysgalactiae* SpoT produced by Meta-BASIC (*19*). The relationship between the two proteins is quite distant; the residue identities between the two families in the aligned portion of Figure 1 range from 7 to 13%. However, the identification of conserved putative metal binding residues throughout the alignment greatly improves confidence in its accuracy as argued previously for phospholipases (*31*). In the SpoT structure (*29*), the two subunits of the dimer are asymmetric and represent alternate states of activity of the *N*-terminal phosphatase domain (used in our modeling) and the downstream synthetase domain. We mainly used the phosphatase-active site domain, employing only a small piece of the inactive domain to model a small AcpH region (residues 59−65 marked with S in Figure 2) that aligns with a disordered portion of the phosphatase-active domain. As shown in Figure 2, both the insertion and deletions (I and D, respectively; see also Figure 1) are positioned such that they are readily accommodated by the fold. As Figure 2 also shows, the extra region present at the *N*-terminus of SpoT (shades of blue ribbon) forms two helices that lie on the surface of the fold such that its absence in ACP phosphodiesterase would have no implications for the overall structural integrity of the fold. Furthermore, the lack of the *N*-terminal region leads to a much more open catalytic site in ACP phosphodiesterase as would be expected because its substrate is a protein and, thus, is much larger than the substrate of the SpoT domain. As Figure 1 shows, the *C*-terminal segments of the AcpH sequences extend past the point at which they may be confidently aligned with the SpoT domain. However, on the basis of the position of the *C*-terminus in the model (Figure 2), we consider it unlikely

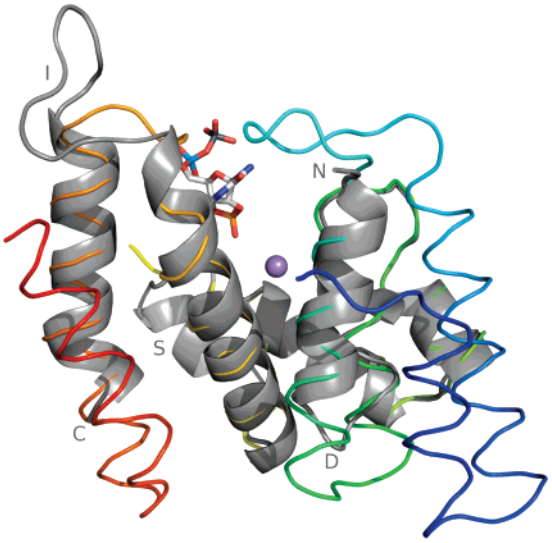

FIGURE 2: Structural alignment of the model of *E. coli* AcpH (gray cartoon) with the *N*-terminal HD phosphatase domain of *S. dysgalactiae* SpoT (ribbon, colored from blue at the *N*-terminus to red at the *C*-terminus). The termini of the model are labeled N and C. As in Figure 1, I and D mark the positions of the major insertion and deletion in AcpH relative to SpoT. S marks the small portion modeled with the aid of the inactive SpoT domain structure (see text). The sphere and stick structures represent the bound metal and ligand (GDP-2′,3′-cyclic monophosphate) of the SpoT structure (*29*). This Figure and Figures 3 and 7 were created with PyMOL (http://pymol.sourceforge.net).

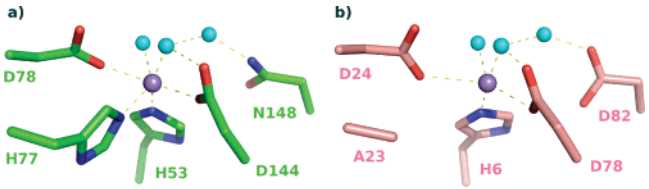

FIGURE 3: Metal binding site of SpoT phosphatase domain (a) compared to the predicted metal site in AcpH (b). In each panel, Mn and nearby water molecules (as seen in the SpoT crystal structure) are shown as violet and cyan spheres, respectively, whereas the dotted lines mark possible hydrogen bonds.

that any of these unmodeled residues contribute to the catalytic site of AcpH.

On the basis of the model, there are no insertions present in AcpH that would disrupt the integrity of the SpoT metal binding site. In our AcpH model, His 6, Asp 24, and Asp 78 contribute to a putative metal binding site in the same manner as the corresponding SpoT domain residues do (Figure 3). Another putative metal binding residue is AcpH residue Asp 82, which aligns with SpoT residue Asn 148 in our model. Asn 148 has a through-water interaction with the bound metal of SpoT, and thus, it seemed plausible that the negative charge of the side chain of AcpH residue Asp 82 could contribute to metal binding. The major difference between the SpoT and modeled AcpH sites is that AcpH lacks a residue corresponding to His 77 of the SpoT sequence. This forms the H of the HD motif that gives rise to the name of the superfamily of phosphatases that includes the SpoT *N*-terminal domain. In the AcpH proteins, small residues, Ala or Gly, occupy the position corresponding to SpoT His 77. The loss of this interaction would be expected to diminish metal binding affinity, and thus, despite our pleasing model, it remained possible that the AcpH active site we had predicted was incorrect. To test this possibility, we modified each of the putative active site residues by site-directed mutagenesis and studied the properties of the purified mutant proteins.

Experimental Tests of the AcpH Model. To test whether or not AcpH residues His6, Asp24, Asp78, and Asp82 are important in metal binding, we constructed mutant genes encoding the hexahistidine-tagged AcpH mutant proteins lacking these residues under the control of the *tac* promoter. By site-directed mutagenesis, His6 was changed to Gln, and each of the three aspartate residues was changed to Asn. In addition, three constructs were made that encoded an *N*-terminally truncated protein lacking the highly conserved residues 2−6, an Ala23 to His mutant protein to give the canonical HD motif and a mutant protein in which both His6 and His8 were substituted with Gln.

As described in Experimental Procedures, strains carrying the constructs described above were cultured and induced for expression and the mutant AcpH proteins were purified. Assays of AcpH activity showed that the mutant proteins had greatly diminished AcpH activities (Figure 4). A low level of AcpH activity was seen in the H6Q and D24N proteins, but no detectable activity was observed with any other mutant proteins either by the gel shift assays (Figure 4) or by assaying [^{3}H]-phosphopantetheine release from [^{3}H]-ACP (data not shown). It is interesting to note that our attempt to produce a protein having the HD motif (the A23H mutant) completely abolished activity. We also found that the weak activity of the H6Q mutant was eliminated by substitution of His8 with Gln. To verify that the *C*-terminal hexahistidine tags were not responsible for loss of activity, *acpH* deletion strains harboring constructs expressing untagged versions of the AcpH mutants were induced for expression, and crude extracts of these strains were assayed for AcpH activity. These extracts showed the same activity pattern as those of the purified enzymes (data not shown). The H6Q and D24N mutant proteins were also assayed with [^{3}*H*]-ACP to determine the dependence of their reaction rates on substrate concentration. As expected, both mutant proteins show reduced affinities for ACP and greatly reduced reaction rates (Figure 5, Table 2). Although the data of Table 2 indicate that the wild-type AcpH is a remarkably slow enzyme, it should be noted that the enzyme remains in a polydisperse aggregated form despite the more efficient refolding given by the use of the proprietary Profoldin

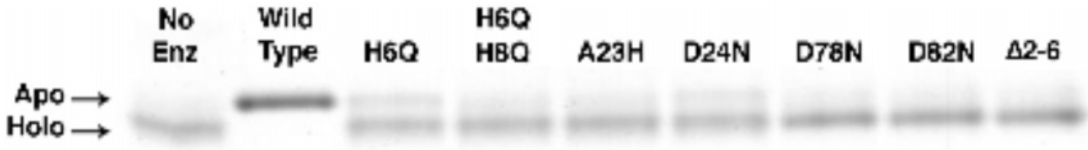

FIGURE 4: Activities of the mutant AcpH proteins in the gel shift assay. The assays were performed with 20 μM ACP, 200 μM $MnCl_2$, and 2.0 pmol of either the wild-type or a mutant AcpH as described in Experimental Procedures. No Enz denotes the control incubation without enzyme. The reaction products were analyzed by electrophoresis on 20% nondenaturing polyacrylamide gels.

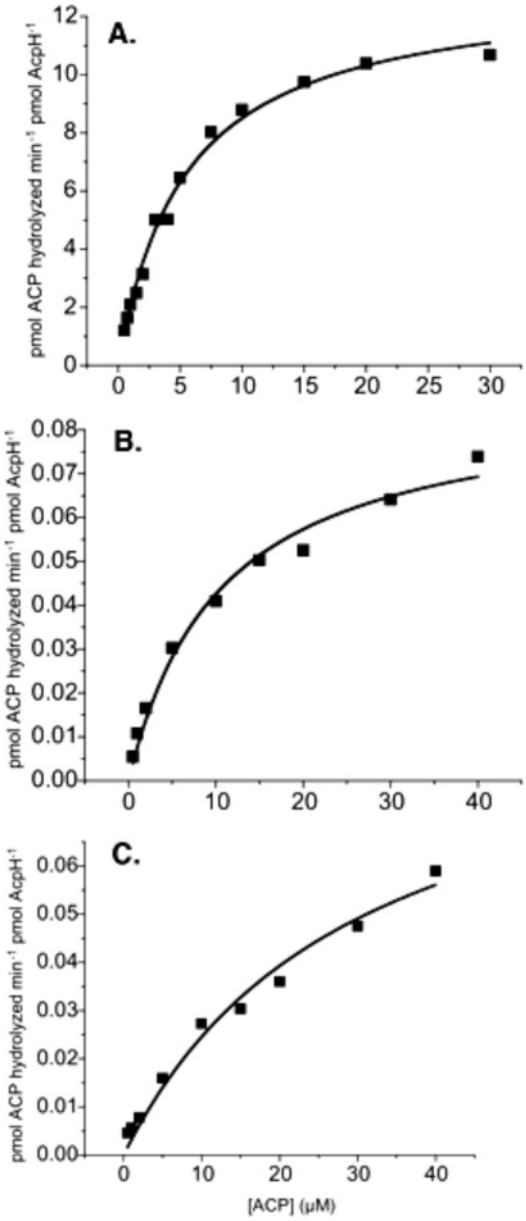

FIGURE 5: ACP phosphodiesterase activities versus the concentration of holo-ACP for the wild type (panel A), AcpH H6Q (panel B), and AcpH D24N proteins obtained by the radioactive assay. The reactions were initiated by the addition of 0.1 pmol of wild-type AcpH in Panel A or 2 pmol of AcpH H6Q or AcpH D24N in Panels B and C, respectively. The reactions were stopped by the addition of trichloroacetic acid, and the soluble fraction was extracted with diethyl ether to remove the acid and then counted for radioactivity.

columns in place of the refolding conditions used previously (*10*). Hence, it remains possible that only a fraction of the enzyme is properly folded and active. It should be noted that our AcpH preparations are absolutely dependent on divalent ions for activity. (The activity seen in the absence of Mn^{2+} in Figure 5 is due to the Mg^{2+} present in the buffer.) With no added metal ions, the basal activity for wild-type AcpH under the otherwise standard reaction conditions, (20 μM ACP and 2 pmol AcpH, 2 h of incubation) was <0.005 pmol ACP min^{-1} $pmol^{-1}$ AcpH. Addition of 10 mM ethylenediaminetetraacetic acid also resulted in undetectable levels of activity.

Elevated Mn^{2+} Concentrations Give Increased Activities of the H6Q and D24N Mutant Proteins. Our model implicated the residues we mutagenized in metal binding, and thus, it seems that increasing the concentration of $MnCl_2$ in the AcpH assay might increase the activities of those mutant enzymes that retained some activity. Indeed, the activities of the H6Q and D24N mutant proteins increased with $MnCl_2$ concentration. However, these mutant enzymes required much higher concentrations of $MnCl_2$ than the wild-type enzyme to achieve their maximal activities (Figure 6). The mutant enzymes required about 5 mM $MnCl_2$ for optimal activity, whereas the wild-type enzyme was largely saturated at 50 μM $MnCl_2$. Increased $MnCl_2$ concentrations had no

Table 2: Kinetic Constants of the Wild-Type and Mutant AcpH Proteins[a]

AcpH protein	K_M (μM)	V_{max} (pmol ACP hydrolyzed min^{-1} $pmol^{-1}$ of AcpH)
wild type	5.4 ± 0.4	13.1 ± 0.4
H6Q	10.6 ± 1.8	0.10 ± 0.01
H6Q H8Q	ND	<0.005
A23H	ND	<0.005
D24N	29.9 ± 7.7	0.10 ± 0.01
D78N	ND	<0.005
D82N	ND	<0.005
Δ(2−6)	ND	<0.005

[a] The assays were performed at 200 μM $MnCl_2$. ND, not determinable.

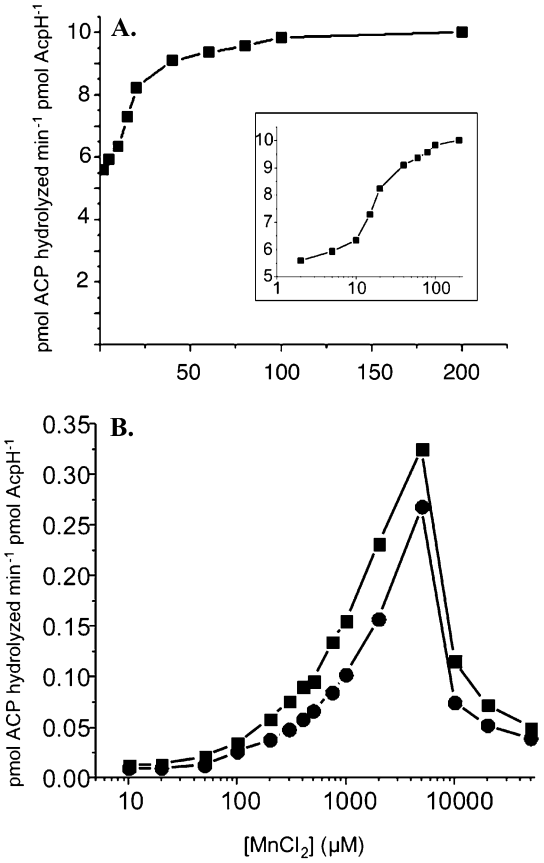

FIGURE 6: Dependence of ACP phosphodiesterase activity on $MnCl_2$ concentration for the wild type (panel A) and AcpH H6Q and AcpH D24N proteins (panel B) obtained using the radioactive assay. In panel B, the symbols denote the following: ■, AcpH H6Q and ●, AcpH D24N. The insert in panel A shows the data with the $MnCl_2$ concentration plotted on a log scale. The activity seen in the absence of added Mn in panel A is due to the $MgCl_2$ (25 mM) present in the buffers (see text). The assays contained 20 μM ACP.

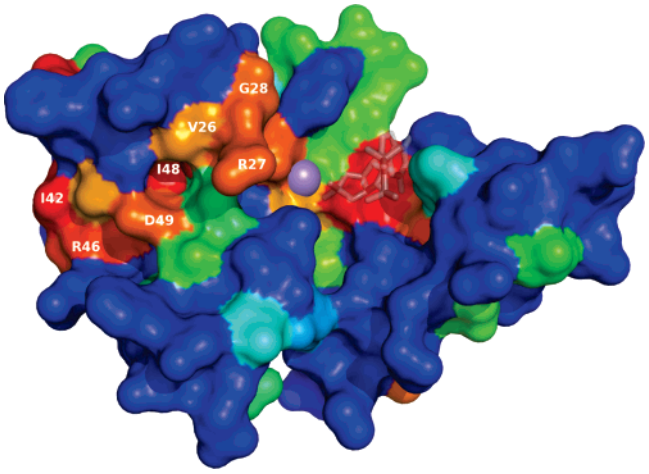

FIGURE 7: Mapping of family sequence conservation onto the modeled *E. coli* AcpH structure. The blue regions are nonconserved, whereas the red regions are the most highly conserved, and other colors mark intermediate degrees of conservation. The sphere and (semi-transparent) ligand are taken from the superimposed SpoT template structure and mark the catalytic site. The residues that contribute to the highly conserved canyon that leads away from the catalytic site are labeled.

detectable effects on the other mutant enzymes. All of the proteins that were inactive at low Mn^{2+} concentrations remained totally inactive at elevated Mn^{2+} concentrations (data not shown).

DISCUSSION

Although AcpH lacks the histidine of the HD motif, the enzymatic activity depends on the other metal binding residues conserved in the HD superfamily of phosphatases and phosphodiesterases. The lack of the signature histidine ligand suggests that AcpH might bind Mn^{2+} more weakly than SpoT. However, the supplement to Hogg et al. (*29*) reports that a mutant SpoT in which alanine was substituted for the histidine of the HD motif retained 26% of the wild-type guanosine-3′,5′-bis(diphosphate) 3′-diphosphatase activity, whereas substitution of alanine for the aspartate of the HD motif resulted in a complete loss of activity, in good agreement with our results for the D24N AcpH. Hence, the histidine of the HD motif is not strictly required for activity, and in the case of AcpH, its introduction destroys activity. However, mutagenesis of other SpoT residues that are not found in AcpH also result in inactive proteins (*29*), suggesting that the cores of the two active sites have evolved significant differences. One of these is an essential SpoT residue, Asn 148, which has a through-water interaction with the bound metal and is replaced by Asp 82 in AcpH. Because Asp 82 is essential for AcpH activity, the negative charge of this AcpH residue might contribute to metal affinity. Another possibility for an additional metal binding ligand (if needed) would be a side chain of the substrate protein. This cannot be a histidine residue because the sole histidine of ACP is located toward the end of the protein about 25 Å from the site of 4′-PP attachment at serine-36 (*32*). However, one of the proximal conserved acidic residues of ACP such as Asp 35 or Asp 38 might contribute to metal binding.

The results of our mutagenesis studies plus the finding that the activities of some mutant proteins are increased by high Mn^{2+} concentrations strengthens our belief that the model depicts the active site of AcpH with reasonable fidelity. We, therefore, have mapped the sequence conservation of the AcpH family onto the model (Figure 7). As expected, residues at and near the metal site are highly conserved. However, a further highly conserved canyon leading away from the catalytic site is clearly evident. We believe that this is likely to represent part of the substrate binding site, perhaps that of the phosphopantetheine moiety (plus the proximal part of any acyl groups attached to the thiol).

REFERENCES

1. Walsh, C. (2005) *Posttranslational Modification of Proteins: Expanding Nature's Inventory*, Roberts and Company, Englewood, CO.
2. Rock, C. O., and Jackowski, S. (2002) Forty years of bacterial fatty acid synthesis, *Biochem. Biophys. Res. Commun. 292*, 1155−1166.
3. Ohlrogge, J. B., and Kuo, T. M. (1985) Plants have isoforms for acyl carrier protein that are expressed differently in different tissues, *J. Biol. Chem. 260*, 8032−8037.
4. Cronan, J. E., Fearnley, I. M., and Walker, J. E. (2005) Mammalian mitochondria contain a soluble acyl carrier protein, *FEBS Lett 579*, 4892−4896.
5. Wada, H., Shintani, D., and Ohlrogge, J. (1997) Why do mitochondria synthesize fatty acids? Evidence for involvement in lipoic acid production, *Proc. Natl. Acad. Sci. U.S.A. 94*, 1591−1596.
6. Waters, N. C., Kopydlowski, K. M., Guszczynski, T., Wei, L., Sellers, P., Ferlan, J. T., Lee, P. J., Li, Z., Woodard, C. L., Shallom, S., Gardner, M. J., and Prigge, S. T. (2002) Functional characterization of the acyl carrier protein (PfACP) and β-ketoacyl ACP synthase III (PfKASIII) from *Plasmodium falciparum*, *Mol. Biochem. Parasitol. 123*, 85−94.
7. Lambalot, R. H., Gehring, A. M., Flugel, R. S., Zuber, P., LaCelle, M., Marahiel, M. A., Reid, R., Khosla, C., and Walsh, C. T. (1996) A new enzyme superfamily - the phosphopantetheinyl transferases, *Chem. Biol. 3*, 923−936.
8. Walsh, C. T., Gehring, A. M., Weinreb, P. H., Quadri, L. E., and Flugel, R. S. (1997) Post-translational modification of polyketide and nonribosomal peptide synthases, *Curr. Opin. Chem. Biol. 1*, 309−315.
9. Vagelos, P. R., and Larrabee, A. R. (1967) Acyl carrier protein. IX. Acyl carrier protein hydrolase, *J. Biol. Chem. 242*, 1776−1781.
10. Thomas, J., and Cronan, J. E. (2005) The enigmatic acyl carrier protein phosphodiesterase of Escherichia coli: genetic and enzymological characterization, *J. Biol. Chem. 280*, 34675−34683.
11. Fischl, A. S., and Kennedy, E. P. (1990) Isolation and properties of acyl carrier protein phosphodiesterase of *Escherichia coli*, *J. Bacteriol. 172*, 5445−5449.
12. Altschul, S. F., Madden, T. L., Schaffer, A. A., Zhang, J., Zhang, Z., Miller, W., and Lipman, D. J. (1997) Gapped BLAST and PSI-BLAST: a new generation of protein database search programs, *Nucleic Acids Res. 25*, 3389−3402.
13. Clamp, M., Cuff, J., Searle, S. M., and Barton, G. J. (2004) The Jalview Java alignment editor, *Bioinformatics 20*, 426−427.
14. Sali, A., and Blundell, T. L. (1993) Comparative protein modelling by satisfaction of spatial restraints, *J. Mol. Biol. 234*, 779−815.
15. Laskowski, R., MacArthur, M., Moss, D., and Thornton, J. (1993) PROCHECK: a program to check the stereochemical quality of protein structures, *J. Appl. Crystallogr. 26*, 283−290.
16. Gouet, P., Courcelle, E., Stuart, D. I., and Metoz, F. (1999) ESPript: analysis of multiple sequence alignments in PostScript, *Bioinformatics 15*, 305−308.
17. Bujnicki, J. M., Elofsson, A., Fischer, D., and Rychlewski, L. (2001) Structure prediction meta server, *Bioinformatics 17*, 750−751.
18. Bujnicki, J. M., Elofsson, A., Fischer, D., and Rychlewski, L. (2001) LiveBench-1: continuous benchmarking of protein structure prediction servers, *Protein Sci. 10*, 352−361.
19. Ginalski, K., von Grotthuss, M., Grishin, N. V., and Rychlewski, L. (2004) Detecting distant homology with Meta-BASIC, *Nucleic Acids Res. 32*, W576−W581.
20. Soding, J. (2005) Protein homology detection by HMM-HMM comparison, *Bioinformatics 21*, 951−960.

21. Soding, J., Biegert, A., and Lupas, A. N. (2005) The HHpred interactive server for protein homology detection and structure prediction, *Nucleic Acids Res. 33*, W244−W248.
22. Jones, D. T. (1999) Protein secondary structure prediction based on position-specific scoring matrices, *J. Mol. Biol. 292*, 195−202.
23. Cherepanov, P. P., and Wackernagel, W. (1995) Gene disruption in Escherichia coli: TcR and KmR cassettes with the option of Flp-catalyzed excision of the antibiotic-resistance determinant, *Gene 158*, 9−14.
24. Datsenko, K. A., and Wanner, B. L. (2000) One-step inactivation of chromosomal genes in Escherichia coli K-12 using PCR products, *Proc. Natl. Acad. Sci. U.S.A. 97*, 6640−6645.
25. Keating, D. H., Carey, M. R., and Cronan, J. E., Jr. (1995) The unmodified (apo) form of Escherichia coli acyl carrier protein is a potent inhibitor of cell growth, *J. Biol. Chem. 270*, 22229−22235.
26. Vogel, H. J., and Bonner, D. M. (1956) Acetylornithinase of Escherichia coli: partial purification and some properties, *J. Biol. Chem. 218*, 97−106.
27. Grana, D., Gardella, T., and Susskind, M. M. (1988) The effects of mutations in the ant promoter of phage P22 depend on context, *Genetics 120*, 319−327.
28. Rawlings, M. (1993) Isolation and Characterization of a Gene and a Genomic Clone Encoding Acyl Carrier Protein from *Escherichia coli*, Ph.D. Thesis, University of Illinois, Urbana−Champaign.
29. Hogg, T., Mechold, U., Malke, H., Cashel, M., and Hilgenfeld, R. (2004) Conformational antagonism between opposing active sites in a bifunctional RelA/SpoT homolog modulates (p)ppGpp metabolism during the stringent response, *Cell 117*, 57−68.
30. Aravind, L., and Koonin, E. V. (1998) The HD domain defines a new superfamily of metal-dependent phosphohydrolases, *Trends Biochem. Sci. 23*, 469−472.
31. Rigden, D. J. (2004) A distant evolutionary relationship between GPI-specific phospholipase D and bacterial phosphatidylcholine-preferring phospholipase C, *FEBS Lett. 569*, 229−234.
32. Roujeinikova, A., Baldock, C., Simon, W. J., Gilroy, J., Baker, P. J., Stuitje, A. R., Rice, D. W., Slabas, A. R., and Rafferty, J. B. (2002) X-ray crystallographic studies on butyryl-ACP reveal flexibility of the structure around a putative acyl chain binding site, *Structure 10*, 825−835.
33. Wertman, K. F., Wyman, A. R., and Botstein, D. (1986) Host/vector interactions which affect the viability of recombinant phage lambda clones, *Gene 49*, 253−262.
34. Jackowski, S., and Rock, C. O. (1981) Regulation of coenzyme A biosynthesis, *J. Bacteriol. 148*, 926−932.
35. Barton, G. J. (1993) ALSCRIPT: a tool to format multiple sequence alignments, *Protein Eng. 6*, 37−40.

BI061789E